Energy Dependence of Photoion Rotational Distributions of N2 and CO

Heung Cheun Choi,[1] R. M. Rao,[1] A. G. Mihill,[2] Sandeep Kakar,[1] E. D. Poliakoff,[3] Kwanghsi Wang,[4] and V. McKoy[4]

[1]Department of Physics and Astronomy, Louisiana State University, Baton Rouge, Louisiana 70803

[2]Center for Advanced Microstructures and Devices, Louisiana State University, Baton Rouge, Louisiana 70803

[3]Department of Chemistry, Louisiana State University, Baton Rouge, Louisiana 70803

[4]Arthur Amos Noyes Laboratory of Chemical Physics, California Institute of Technology, Pasadena, California 91125

(Received 2 September 1993)

We present the first measurements of rotational distributions for photoionization over extended energy ranges [$0 \leq E_k \leq 200$ eV for N2 ($2\sigma_u^{-1}$) and of $3 \leq E_k \leq 125$ eV for CO ($4\sigma^{-1}$)]. The N2 and CO results show a strikingly unusual and different energy dependence. Although differences are expected due to the absence of a center of symmetry in CO, detailed calculations reveal that this behavior arises from the presence of Cooper minima in the photoelectron continuum ($k\sigma_g$) in the case of N2 and from an f-wave shape resonance for $4\sigma^{-1}$ photoionization in CO.

PACS numbers: 33.80.Eh, 33.10.Ev, 33.50.Dq

Rotationally resolved molecular photoionization is a topic of intense current interest [1–13] due to the valuable insight that such highly resolved data provide into the underlying dynamics of these processes. In particular, rotational resolution provides a window on the angular momentum composition of the photoelectron and on the partitioning of angular momentum between the photoelectron and ion core. However, rotationally resolved studies have been restricted to threshold or near-threshold ionization phenomena. In this Letter we present results of measurements of rotational distributions over an extended energy range for the first time [$0 \leq E_k \leq 200$ eV for N2 ($2\sigma_u^{-1}$) and $3 \leq E_k \leq 125$ eV for CO ($4\sigma^{-1}$)], which show a strikingly unusual and different dependence on photoelectron kinetic energy. Detailed calculations of these ion distributions reveal that this behavior arises from the presence of Cooper minima in the photoelectron continuum ($k\sigma_g$) in the case of N2 and of an f-wave shape resonance for 4σ photoionization in CO [14]. These results demonstrate that rotationally resolved fluorescence can probe aspects of ionization dynamics that are not accessible from alternative measurements and that the energy dependence of these distributions can extend deep into the ionization continua.

The earliest rotationally resolved photoionization data were obtained via photoelectron spectroscopy of H2 using resonance lamp excitation [1]. There has been increasing interest as a result of experimental innovations with both lasers and photoelectron spectroscopy. Examples include photoelectron spectroscopy following resonance enhanced multiphoton ionization (REMPI) [3,5–7], laser-induced fluorescence following REMPI [8], and zero-kinetic-energy pulsed-field-ionization (ZEKE-PFI) spectroscopy [2,9,10]. These studies have demonstrated that, while parity selection rules constrain the angular momentum of the photoelectron-photoion complex, such spectra provide useful fingerprints of the partitioning of angular momentum between the electron and ion [4,11]. For single-photon ionization, conservation of angular momentum re-

stricts [4] ΔJ to

$$\Delta J = J^+ - J_0 = l + \tfrac{3}{2}, l + \tfrac{1}{2}, \ldots, -(l + \tfrac{3}{2}). \quad (1)$$

For example, an $l = 3$ (i.e., an f-wave) component of the photoelectron can lead to angular momentum changes as large as $\Delta J = \tfrac{9}{2}$ or $\Delta N = 4$, excluding electron spin. The actual ΔN values that occur depend sensitively on microscopic aspects of the scattering dynamics. Ion rotational distributions can be strongly influenced by off-diagonal contributions ($l \neq l'$) to the photoelectron matrix elements $r_{fi}^{l\lambda\mu}$

$$r_{fi}^{l\lambda\mu} = \sum_{l',l_0} \langle g_{lm,l'\lambda}(k,r) Y_{l'\lambda}(\hat{f}') | r Y_{1\mu}(\hat{f}') | \phi_{il_0}(r) Y_{l_0\lambda_0}(\hat{f}') \rangle, \quad (2)$$

which arise from angular momentum changing collisions of the photoelectron with the ion core. In Eq. (2) $g_{lm,l'\lambda}(kr)$ and ϕ_{il_0} are components of single-center expansions of the photoelectron wave function $\psi_{klm}^{(-)}(\mathbf{r})$ and the initial orbital $\phi_i(\mathbf{r}')$, respectively, λ is the projection of l along the internuclear axis, and μ is the photon polarization index in the molecular frame. Data over a wide energy range can be particularly useful in illustrating qualitative aspects of such underlying dynamical behavior [12]. However, this requirement of extensive spectral coverage presents serious obstacles in studies of rotationally resolved photoelectron spectra. With rotational energy spacings on the order of 4 cm^{-1} (500 μeV), even for favorable diatomic systems, rotationally resolved photoelectron spectra at $h\nu_{exc} = 220$ eV require a resolving power of 10^6, which is orders of magnitude beyond the limits of the highest resolution photoelectron spectroscopy at comparable energies [15,16].

We demonstrate that rotationally resolved data can be accessed over the necessary range by detecting dispersed fluorescence from excited photoions, confirming technical advantages that have been demonstrated in earlier high resolution ionization studies [17,18]. In the present study, neutral gas-phase molecules are ionized by mono-

chromatized synchrotron radiation and we measure the intensities of rotationally resolved fluorescence transitions from electronically excited levels of N_2^+ and CO^+ photoions. Because we observe fluorescence, *the detection bandwidth is uncoupled from and therefore not limited by the excitation bandwidth* [17], permitting us to exploit the broad tunability of synchrotron radiation. The excitation and fluorescence sequence is the same as used previously [18]; i.e., neutral N_2 molecules are photoionized and the dispersed fluorescence, $N_2^+(B^2\Sigma_u^+, v^+ = 0, N^+)$ $\rightarrow N_2^+(X^2\Sigma_g^+, v'' = 1, N'') + h\nu_{N^+N''}$, is monitored. The CO measurements are analogous. For N_2 data were generated over the range $20 \le h\nu_{exc} \le 220$ eV but, with its lower signal intensities, results were only obtained from $23 \le h\nu_{exc} \le 145$ eV for CO. Synchrotron radiation from the Louisiana State University Center for Advanced Microstructures and Devices (CAMD) facility [19] is monochromatized ($\Delta h\nu_{exc} \approx 600$ meV) by a 6-m plane grating monochromator [20] and ionizes the target molecules. The fluorescence is dispersed and detected as described previously [17,18]. To limit the number of target states, the target molecules were rotationally cooled in a supersonic expansion [21-23]. Data were obtained over a range of stagnation pressures to test for secondary processes, such as ionization induced by secondary photoelectrons. These tests showed the data to be free of secondary artifacts [21]. We also verified that the excitation photon beam position did not vary with energy, which could result in a changing distribution of target states. A comprehensive discussion of the experimental details will be given elsewhere [21].

Figure 1 shows photoion fluorescence spectra for N_2 at photon energies of 40 and 192 eV. The intensities of
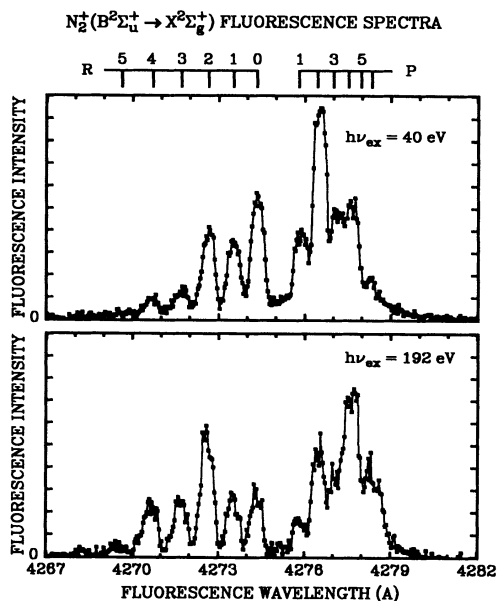
transitions originating from rotational levels of the ion are dramatically different at these two energies, reflecting the changing rotational distributions of the photoions. To obtain the rotational distributions, we determine the population of each level, n_{N^+}, from the relative fluorescence intensities, as described elsewhere [18,21]. Fluorescence spectra were obtained at least every 10 eV. At lower energies, a finer energy mesh was used. These measured ionic rotational populations $(n_{N^+}/\Sigma n_{N^+})$ are normalized and plotted as a function of photon energy in Fig. 2. The data are not corrected for differences in rotational alignments, but alignment effects are not expected to alter the relative fluorescence intensities significantly [23]. The changes in the rotational distributions are clearly significant over the photon energy of Fig. 2. As the energy increases, population is transferred from low N^+ levels to higher ones, due to the increasing propensities for larger ΔN transitions. For the weakly populated $N^+ = 5$ level, the relative populations increase by more than a factor of 4 over the energy range of Fig. 2, while the $N^+ = 1$ population falls by a factor of 2.

Results of analogous measurements of ion rotational distributions for CO are also shown in Fig. 2. In contrast to the N_2 results, these CO^+ distributions show essentially no dependence on energy. This difference in the ion rotational distributions for these two isoelectronic systems over such a broad energy range is quite unexpected. Studies of the underlying dynamics responsible for this difference in behavior are clearly desirable.

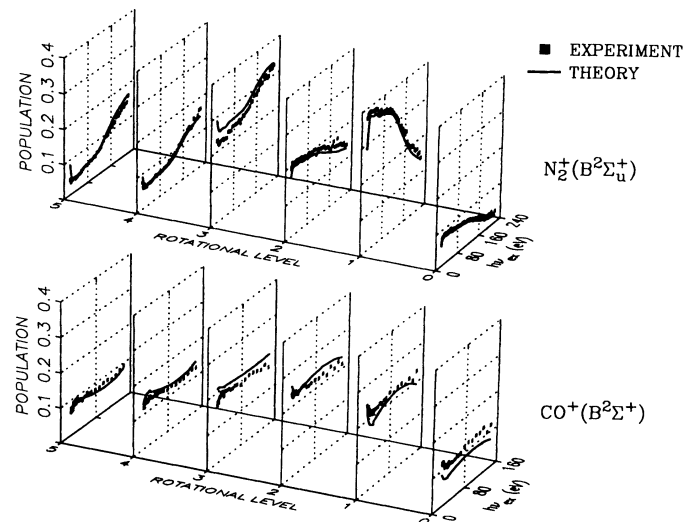Figure 2 also shows our calculated ion rotational distri-

FIG. 2. Top: Calculated and measured rotationally resolved photoion distributions for photoionization of the $2\sigma_u$ orbital of the ground $X^1\Sigma_g^+$ state of N_2 leading to the excited $B^2\Sigma_u^+$ state of N_2^+ by synchrotron radiation. Bottom: Calculated and measured rotationally resolved photoion distributions for photoionization of the 4σ orbital of the ground $X^1\Sigma^+$ state of CO leading to the excited $B^2\Sigma^+$ state of CO^+ by synchrotron radiation.

FIG. 1. Rotationally resolved fluorescence spectra of $N_2^+(B^2\Sigma_u^+)$ photoions.

butions for photoionization of the $2\sigma_u$ and 4σ orbitals of N_2 and CO, respectively. The calculations are performed at the Hartree-Fock level [21,24], and the photoelectron orbitals are obtained by numerical solution of the Lippmann-Schwinger equations using an iterative procedure, based on the Schwinger variational principle [24]. Details will be given elsewhere [21]. The calculated spectra for N_2 and CO assumed temperatures of 14 and 18 K, respectively. Agreement between the calculated and measured spectra is generally excellent.

To gain insight into the underlying dynamical behavior of these ion distributions, we examine the dependence of the angular momentum composition of the photoelectron matrix elements on kinetic energies. Analysis of the photoelectron matrix elements of Eq. (2) for photoionization of the $2\sigma_u$ orbital of the ground state of N_2 reveals that Cooper minima, which are due to sign changes in the photoelectron matrix elment, occur in the d wave ($l=2$) at $E_k \approx 120$ eV ($h\nu_{exc} \approx 140$ eV) and in the g wave ($l=4$) at $E_k \approx 80$ eV ($h\nu_{exc} \approx 100$ eV) of the $K\sigma_g$ electronic continuum [21]. Since formation of these Cooper minima depletes the d ($l=2$) and g ($l=4$) continuum waves, the lower s wave ($l=0$) of the $k\sigma_g$ channel dominates, resulting in lower ΔJ (ΔN) transitions. Furthermore, this analysis shows that the magnitude of the g waves in the $k\sigma_g$ and $k\pi_g$ continua is comparable to those of the s and d waves at larger kinetic energies (e.g., $E_k > 150$ eV). This behavior reflects the coupling of angular momentum in the photoelectron continuum due to torques associated with the nonspherical molecular ion potential and cannot be explained on the basis of an atomiclike propensity rule for photoionization of this $2\sigma_u$ orbital with its 90.7% p, 6.7% f, and 1.5% h ($l_0=5$) character. These higher l components of the photoelectron matrix element, in turn, lead to larger ΔN transitions, on the basis of the parity selection rule of $\Delta N + l = $odd [4,11] and Eq. (1). This change from smaller to larger ΔN transitions due to the Cooper minima and the contributions of the higher l waves provides an explanation of the trend observed in photoion rotational distributions of Fig. 2 for N_2. Note that symmetry precludes odd photoelectron partial waves and, hence, no $\Delta N = $even transitions occur for N_2 $2\sigma_u^{-1}$ photoionization.

The behavior of the photoelectron matrix elements for photoionization of the 4σ orbital of the ground state of CO differs significantly from that of N_2. There is an f-wave shape resonance [14,25] peaking at $E_k \approx 19$ eV in the $k\sigma$ continuum and a broad enhancement of the $f\pi$ wave peaking at $E_k \approx 30$ eV. On the other hand, the effect of any Cooper minima is much less evident here than in the N_2 system. Further details will be discussed elsewhere [21]. This large $l=3$ contribution to the photoelectron matrix element [21] results in larger ΔN transitions at the lower end of the energy range than expected while other higher partial waves sustain this trend at higher energies. Thus, the f-wave shape resonance in the

$k\sigma$ channel and the enhancement of the f wave in the $k\pi$ channel are responsible for the flat behavior seen in the CO^+ rotational distributions of Fig. 2. Small features in both the measured and calculated ion rotational distributions at photon energies between 37 and 40 eV are due to this f-wave shape resonance [21,26]. These f-wave enhancements are molecular in origin since the 4σ orbital of CO with its 14.6% s, 62.3% p, 15.7% d, 3.1% f, and 2.7% g ($l_0=4$) character is expected to lead to dominant s and d waves on the basis of atomiclike propensity rules.

These results demonstrate that rotationally resolved photoion fluorescence complements existing laser-based photoelectron and induced fluorescence methods [2-11, 13]. Moreover, the current data are also complementary to synchrotron-based rotationally unresolved determinations, such as photoelectron angular distributions, which are also sensitive to Cooper minima and shape resonances. A fuller discussion of the information content of the rotationally resolved measurements will be provided elsewhere [21]. With its broad spectral range, dispersed fluorescence measurements are highly suitable for survey studies that can characterize molecular photoionization dynamics. The present results for N_2 demonstrate that rotational distributions can display dynamically significant behavior, even at high photoelectron energies, due to the presence of Cooper minima and l mixing arising from the nonatomiclike character of the molecular photoelectron [21]. Such effects of Cooper minima, shape resonances, and strong l mixing in the electronic continua on the ion rotational distributions have been observed in other diatomic molecules [2,3,8,11]. The present studies of photoion rotational distributions of N_2 and CO serve to illustrate such effects at energies well beyond the reach of conventional photoelectron spectroscopy.

[1] See, for example, L. Åsbrink, Chem. Phys. Lett. 7, 549 (1970); A. Niehaus and M. W. Ruf, Chem. Phys. Lett. 11, 55 (1971); E. S. Chang, J. Phys. B 11, L69 (1978); Y. Itikawa, Chem. Phys. 37, 401 (1979); J. E. Pollard, D. J. Trevor, J. E. Reutt, Y. T. Lee, and D. A. Shirley, J. Chem. Phys. 77, 34 (1982); D. Dill, Phys. Rev. A 6, 160 (1972).

[2] M. Braunstein, V. McKoy, S. N. Dixit, R. G. Tonkyn, and M. G. White, J. Chem. Phys. 93, 5345 (1990); R. G.

Tonkyn, J. W. Winniczek, and M. G. White, Chem. Phys. Lett. **164**, 137 (1989).

[3] E. de Beer, C. A. de Lange, J. A. Stephens, K. Wang, and V. McKoy, J. Chem. Phys. **95**, 714 (1991); K. Wang, J. A. Stephens, V. McKoy, E. de Beer, C. A. de Lange, and N. P. C. Westwood, J. Chem. Phys. **97**, 211 (1992); K. Wang, J. A. Stephens, and V. McKoy, J. Chem. Phys. **95**, 6456 (1991).

[4] J. Xie and R. N. Zare, J. Chem. Phys. **93**, 3033 (1990).

[5] X. Song, E. Sekreta, J. P. Reilly, H. Rudolph, and V. McKoy, J. Chem. Phys. **91**, 6062 (1989).

[6] K. L. Reid, D. J. Leahy, and R. N. Zare, Phys. Rev. Lett. **68**, 3527 (1992).

[7] S. T. Pratt, P. M. Dehmer, and J. L. Dehmer, J. Chem. Phys. **78**, 4315 (1983).

[8] J. Xie and R. N. Zare, Chem. Phys. Lett. **159**, 399 (1989).

[9] K. Müller-Dethlefs and E. W. Schlag, Annu. Rev. Phys. Chem. **42**, 109 (1991).

[10] M.-T. Lee, K. Wang, V. McKoy, R. G. Tonkyn, R. T. Wiedmann, E. R. Grant, and M. G. White, J. Chem. Phys. **96**, 7848 (1992).

[11] K. Wang and V. McKoy, J. Chem. Phys. **95**, 4977 (1991).

[12] R. T. Wiedmann, M. G. White, K. Wang, and V. McKoy, J. Chem. Phys. **98**, 7673 (1993).

[13] A. Strobel, I. Fischer, J. Staeker, G. Nieder-Schatteburg, K. Müller-Dethlefs, and V. Bondybey, J. Chem. Phys. **97**, 2332 (1992).

[14] J. L. Dehmer and D. Dill, Phys. Rev. Lett. **35**, 213 (1975); A. Görling and N. Rösch, J. Chem. Phys. **93**,

5563 (1990).

[15] C. T. Chen, Y. Ma, and F. Sette, Phys. Rev. A **40**, 6737 (1989).

[16] J. D. Bozek, G. M. Bancroft, J. N. Cutler, and K. H. Tan, Phys. Rev. Lett. **65**, 2757 (1990); J. D. Bozek, G. M. Bancroft, and K. H. Tan, Phys. Rev. A **43**, 3597 (1991).

[17] E. D. Poliakoff, *Vacuum Ultraviolet Photoionization and Photodissociation of Molecules and Clusters*, edited by C. Y. Ng (World Scientific, Singapore, 1991).

[18] S. Kakar, H. C. Choi, and E. D. Poliakoff, J. Chem. Phys. **97**, 6998 (1992); E. D. Poliakoff, J. C. K. Chan, and M. G. White, J. Chem. Phys. **85**, 6232 (1986).

[19] B. C. Craft, M. Feldman, E. Morikawa, E. D. Poliakoff, V. Saile, J. D. Scott, and R. L. Stockbauer, Rev. Sci. Instrum. **63**, 1561 (1992).

[20] E. Morikawa, J. D. Scott, E. D. Poliakoff, R. L. Stockbauer, and V. Saile, Rev. Sci. Instrum. **63**, 1300 (1992).

[21] K. Wang, V. McKoy, H. C. Choi, R. Rao, A. G. Mihill, S. Kakar, and E. D. Poliakoff (to be published).

[22] R. E. Smalley, L. Wharton, and D. H. Levy, J. Chem. Phys. **11**, 4977 (1975).

[23] E. D. Poliakoff, J. L. Dehmer, D. Dill, A. C. Parr, K. H. Jackson, and R. N. Zare, Phys. Rev. Lett. **46**, 907 (1981); J. A. Guest, K. H. Jackson, and R. N. Zare, Phys. Rev. A **28**, 2217 (1983).

[24] R. R. Lucchese, G. Raseev, and V. McKoy, Phys. Rev. A **25**, 2572 (1982).

[25] E. W. Plummer, T. Gustafsson, W. Gudat, and D. E. Eastman, Phys. Rev. A **15**, 2339 (1977).

[26] S. Kakar, H. C. Choi, and E. D. Poliakoff, Chem. Phys. Lett. **190**, 489 (1992).